J Solid State Electrochem (2006) 10: 434–438
DOI 10.1007/s10008-005-0009-7

ORIGINAL PAPER

M. S. Bhuvaneswari · S. Selvasekarapandian
O. Kamishima · J. Kawamura · T. Hattori

Structural and impedance analysis of $LiBiP_2O_7$

Received: 16 December 2004 / Revised: 17 January 2005 / Accepted: 09 May 2005 / Published online: 15 July 2005

Abstract A new material $LiBiP_2O_7$ was prepared by solid-state reaction method. The XRD analysis confirms the formation of the sample. The Raman analysis indicates the presence of characteristic bands for a $(P_2O_7)^{4-}$ group in the sample. The electrical characterization was carried out using the impedance spectroscopy method in the frequency range of 1 KHz–5 MHz. The bulk conductivity of the material was extracted from the impedance analysis and was found to be in the order of $10^{-7}\ \Omega^{-1}\ cm^{-1}$ at 473 K. The activation energy was calculated from the Arrhenius plot and was found to be 0.37 eV. The modulus peak maximum shifts to higher frequencies with an increase in temperature and the broad nature of the peaks indicates the non-debye nature of the material. The high value for the activation energy calculated from the conductance spectrum indicates that some energy has been utilized in the creation of charge carriers.

Keywords $LiBiP_2O_7$ · XRD analysis · Raman analysis · Impedance analysis · Arrhenius plot · Modulus analysis · Conductance spectra analysis

Introduction

During the last few years, numerous studies on lithium-ionic conductors have been published [1, 2]. Lithium-ion conducting materials such as $Li_xLa_xTiO_3$, $Li_2BaP_2O_7$, $LiNiVO_4$, and $LiMn_2O_4$ were destined to be used both as solid electrolytes and as electrode materials for secondary batteries because of their significant ionic conductivity, high reduction potential, and the low atomic mass of lithium [3, 4]. Among the lithium-ion conductors, diphosphate material has gained much interest as solid electrolytes for high-energy density batteries, promising non-linear optic materials, ion exchange materials etc. [5]. This is because of the properties of complex monophosphate and diphosphate ions, which have been used as building blocks for a wide variety of crystal phases with a wide spectrum of physical and chemical properties, such as high chemical stability at ambient temperature and high ionic conductivity [6]. Recently Daniela et al. [6] reported synthesis and ionic conductivity studies on cobalt-substituted $LiBaP_2O_7$. But the main disadvantage of this material is its low ionic conductivity. To improve the ionic conductivity of lithium-based phosphate materials, a material search is still necessary and this includes ceramic crystalline materials. In this study, a new material $LiBiP_2O_7$ was synthesized by the solid-state reaction method and was analyzed by XRD, Raman, and impedance spectroscopic techniques.

M. S. Bhuvaneswari · S. Selvasekarapandian (✉)
Solid State and Radiation Physics Laboratory,
Department of Physics, Bharathiar University,
Coimbatore, 641 046 India
E-mail: sekarapandian@yahoo.com
Tel.: +91-422-2422222
Fax: +91-422-2422387

O. Kamishima · J. Kawamura · T. Hattori
Institute of Multidisciplinary Research for Advanced Materials,
Tohoku University, Sendai, Japan

Experimental

The sample $LiBiP_2O_7$ was prepared by the solid-state reaction method. Stoichiometric amounts of the raw materials Li_2CO_3, Bi_2O_3, and $(NH_4)_2HPO_4$ according to the compositions of $LiBiP_2O_7$ were ground into a fine powder using a mortar and pestle. The resultant powder was heated at a temperature of 1,073 K in a silica crucible. The resultant sample was cooled slowly, crushed into fine powders, and then sprayed in a die. A pressure around 4,000 kg cm^{-3} was applied to form the pellet with a thickness of 0.1 cm and a diameter of 1.0 cm. The pellet was sintered at 773 K in air for 1 h. An X-ray diffractogram was taken to confirm the formation of the sample, using the Philips X-ray diffractometer PW 1830. Raman spectra of the samples were obtained by a

microscopic Raman spectrometer using an Ar-ion laser line of 4,880 Å. Lorentzian line shapes were fitted to the Raman spectra from which the peak position was obtained. The impedance analyzer HIOKI 3532 controlled by a computer was used to obtain the electrical measurements in the frequency range of 1 KHz to 5 MHz with silver as an electrode. The ac impedance measurements were made in the temperature range of 423–473 K

Results and discussion

XRD analysis

Figure 1 shows the XRD spectra of $LiBiP_2O_7$. The diffractogram reveals the formation of the crystalline phase of the product. The diffraction peaks were compared with the standard XRD data given by the JCPDS record (28-0555) [7] and were found to match well with the standard data. The standard d spacing and the calculated d spacing are been given in Table 1. The comparison of the observed and standard d spacing indicates the formation of crystalline $LiBiP_2O_7$.

Raman analysis

Figure 2 shows the Raman spectra of $LiBiP_2O_7$. The diphosphate ion consists of two PO_4 tetrahedra with a central P–O–P bridge bond [8]. The bands observed in Raman spectra in the region 563–343 cm^{-1} were assigned to asymmetric (υ_4) and symmetric (υ_2) bending vibrations of PO_4 tetrahedra [9]. For $LiBiP_2O_7$ these bands were observed at 551 and 387 cm^{-1} due to the asymmetric and symmetric bending modes of PO_4 tetrahedra, respectively. Generally the bending modes of the PO_2^{2-} group and the bridge stretching modes of P–O–P were assigned in the regions of 492–412 cm^{-1} and 975–600 cm^{-1}, respectively [8, 9]. The bending modes of PO_2^{2-} for $LiBiP_2O_7$ were observed at 485 cm^{-1}. The P–O–P symmetric and asymmetric stretching vibrations were observed as a weak intensity band at 737 cm^{-1} along with a shoulder peak at

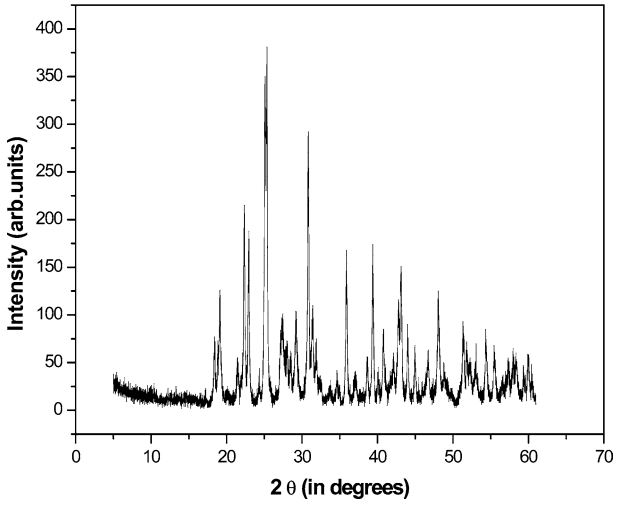

Fig. 1 XRD pattern of $LiBiP_2O_7$ at room temperature

Table 1 Powder XRD data of $LiBiP_2O_7$ at room temperature

2θ (°)	*d* (Å) Experimental	*d* (Å) Standard
19.14	4.63	4.61
21.61	4.10	4.18
22.96	3.87	4.05
25.34	3.51	3.52
27.55	3.23	3.09
29.17	3.05	2.98
30.82	2.89	2.89
34.83	2.57	2.71
36.91	2.43	2.40
39.37	2.28	2.30
41.04	2.19	2.17
43.97	2.05	2.10
45.36	1.99	2.00
48.06	1.89	1.84
51.57	1.77	1.75
57.96	1.58	1.61

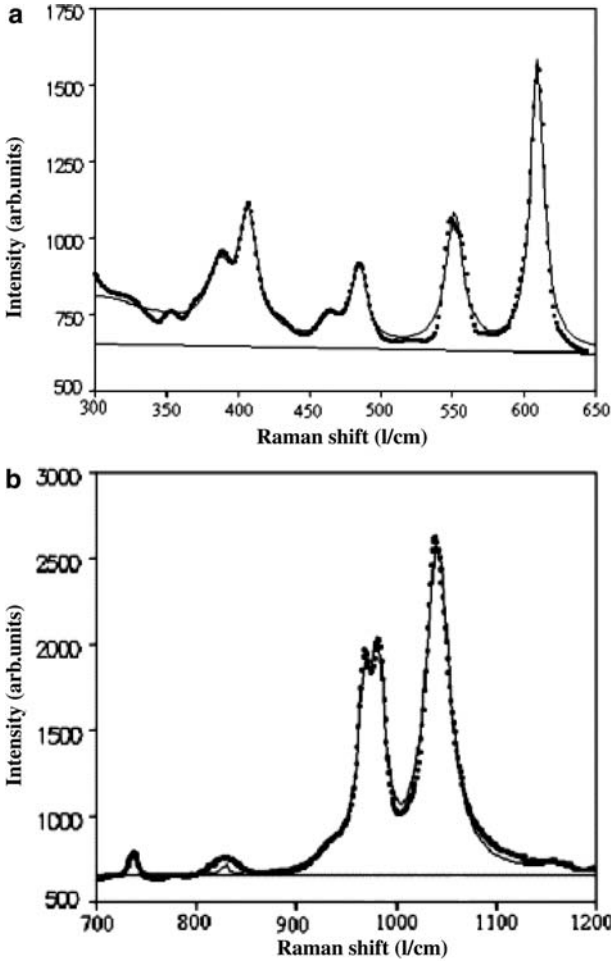

Fig. 2 Raman vibrational spectrum of $LiBiP_2O_7$

945 cm^{-1}. The double peak observed at 967 cm^{-1} was also assigned to the P–O–P asymmetric stretching vibrations. The high intensity band observed at 1,041 cm^{-1} was assigned to stretching modes of PO_4 tetrahedra [10]. The band assignments are shown in Table 2.

Impedance spectroscopy

Figure 3 shows the complex impedance plot for $LiBiP_2O_7$ at 473 K. The data fall on a single semicircle whose center lies below the real axis. The high frequency semicircle was due to the parallel combination of bulk resistance (R_b) and bulk capacitance (C_b) of the $LiBiP_2O_7$. The associated capacitance values were calculated at the arc maximum frequency using the relation $2\pi f_{max}RC = 1$. The observed semicircle has a capacitance of the order of pF and it has been attributed to a conduction process through the bulk or grain interior response of the material, i.e., Li motion within the structure [11].

Bulk resistance values were obtained from the low-frequency intercept of the semicircle on the real Z' axis using the program EQ developed by Boukamp [12, 13]. The bulk conductivity calculated from the formula $1/R \times (l/A)$ was found to be in the order of 10^{-7} Ω^{-1} cm^{-1}. The temperature dependence of bulk conductivity is shown in Fig. 4 and it is found to obey the Arrhenius equation given by

$$\sigma = \sigma_0 e^{-(E_a/KT)} \quad (1)$$

where σ_0 is the pre-exponential factor, E_a is the activation energy. The activation energy was found to be 0.37 eV.

Table 2 Raman spectral data and band assignments of $LiBiP_2O_7$

Raman wave number (cm^{-1})	Assignment
387	υ_2 PO_4
407	Bending modes of P–O–P bridge
465	υ_2 PO_4
485	υ_2 PO_4
551	υ_4 PO_4
609	Symmetric P–O–P stretching
737	Symmetric P–O–P stretching
828	–
943	Assymmetric P–O–P stretching
967	Assymmetric P–O–P stretching
1,041	Symmetric stretching of PO_4

Modulus spectra analysis

The electric modulus formalism has been widely used in glass and ceramic materials because it gives information about the bulk or grain interior response and is not usually affected by blocking phenomena, i.e., grain boundary and electrode response [14]. In order to ascertain whether the arc observed in the impedance analysis has been affected by a grain boundary response overlapped with the grain interior one, an analysis of the imaginary part of the electric modulus as a function of frequency was made. Fig. 5 shows the plot of the imaginary part of the electric modulus (M''/M''_{max}) as a function of frequency indicating an asymmetric peak whose position has been shifted towards higher frequencies with rising temperature. The experimental frequency data are fitted to the equations $f = f_0 \exp(-E_f/Kt)$ [6]. The activation energy E_f has been found to be 0.37 eV. The similar values of E_a and E_f suggest that the impedance arcs were dominated by the grain interior response; hence the conduction in the material is due to Li^+ ions within the structure [14].

Conductance spectra analysis

The frequency dependence of the real part of conductivity for $LiBiP_2O_7$ is shown in Fig. 6. Conductivity has a low frequency plateau and a crossover to power-law

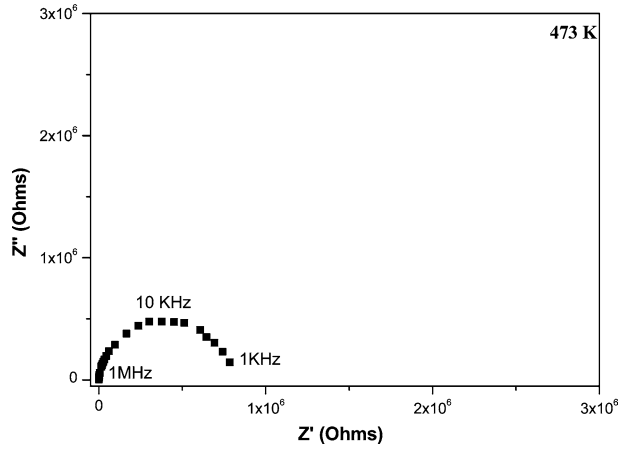

Fig. 3 Complex impedance spectra for $LiBiP_2O_7$ at 473 K

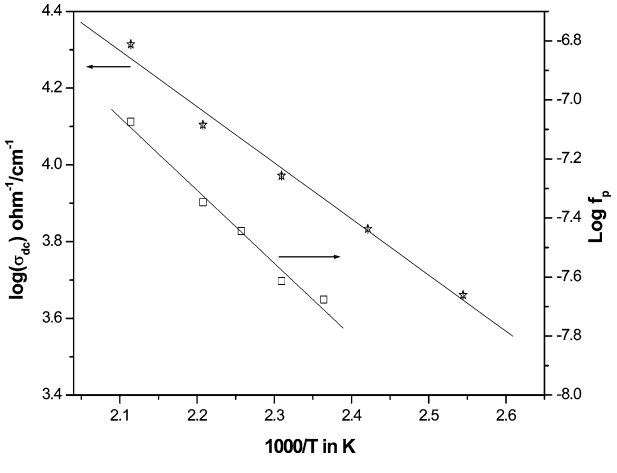

Fig. 4 Temperature dependence of bulk conductance and relaxation frequency for $LiBiP_2O_7$

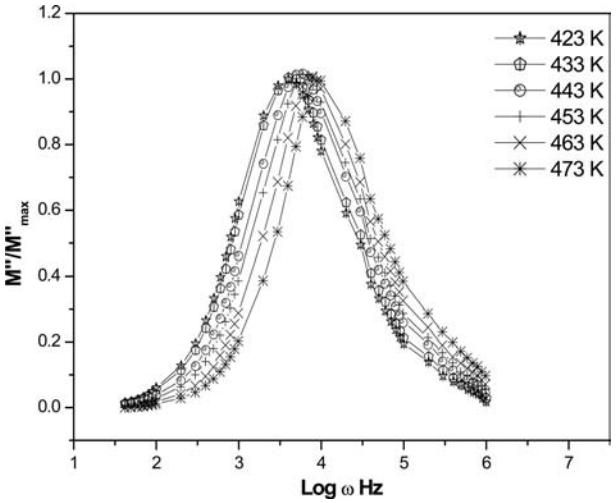

Fig. 5 Normalized modulus M'' spectra for $LiBiP_2O_7$ at various temperatures

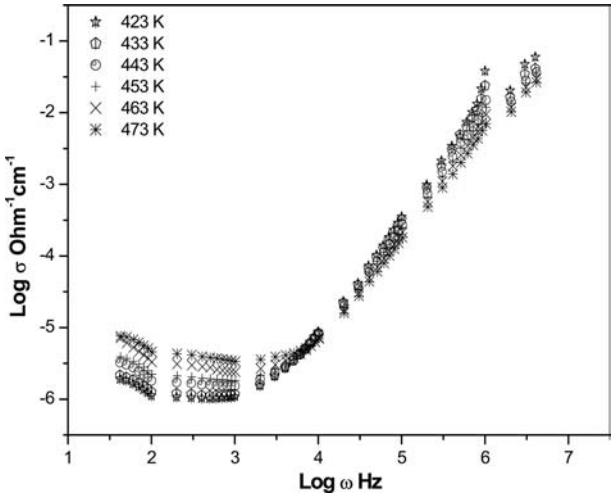

Fig. 6 Conductance spectra for $LiBiP_2O_7$ at various temperatures

dependence at higher frequencies. Conductivity spectra of ionic conductors were found to exhibit universal power law behavior in the form

$$\sigma\prime = \sigma_{dc}[1 + (f/f_p)^{\alpha}] \quad (2)$$

where σ' is the real part of complex conductivity, σ_{dc} is the dc conductivity, f_p is the cross-over frequency, f is the measuring frequency, and α is the exponent of the power law [15–18]. Almond et al. [19] have suggested that the ac conductivity data reveal necessary information on ion dynamics, the cross-over frequency and the exponent provide information on the mobility and the coulomb interaction between mobile ions, respectively. Ionic hopping rates (ω_p) were calculated from the conductivity spectra for all the samples at different temperatures using the formula proposed by Almond and West [17]:

$$\omega_p = 2\sigma_{dc} \quad (3)$$

The calculated hopping frequency was found to be linear with temperature and this variation was fitted to the equation

$$\omega_p = \omega_0 e^{(-E_\omega/Kt)} \quad (4)$$

where ω_0 is the true attempt frequency and E_ω is the activation energy for the hopping process. The activation energy was calculated to be 0.44 eV. This is close to the dc conductivity activation energy (E_a), 0.37 eV. The value of E_ω is somewhat higher than the value of E_a. This indicates that some energy has been utilized for the creation of a free-charge carrier [20]. The activation energies calculated from impedance, modulus, and conductance spectra analysis were found to be low. But the ionic conductivity was not found to be very high. This may be due to the hindrance given by Bi^{3+} ions to Li ions.

Conclusion

The compound $LiBiP_2O_7$ was prepared by solid-state reaction method. The formation of the sample was confirmed by XRD analysis. The Raman analysis indicates the presence of characteristic bands for a $(P_2O_7)^{4-}$ group in the sample. The bulk conductivity calculated from the impedance analysis was found to be $1.5\times10^{-7}\ \Omega^{-1}\ cm^{-1}$ at 473 K. The modulus peak maximum shifts to a higher frequency with an increase in temperature and the broad nature of the peaks indicates the non-debye nature of the material. The similar values for the activation energies E_a and E_f indicate that the grain interior response of the sample alone was observed in the measured frequency range. The low conductivity observed for the sample may be due to the non-availability of vacancy sites for lithium-ion conduction in $LiBiP_2O_7$.

References

1. Catti M, Morgante N, Ibberson RM (2000) J Solid State Chem 152:340–347
2. Rousse G, Wurm C, Morcrette M, Carvajal JR, Gaubicher J, Masquelier C (2001) Int J Inorg Mater 3:881–887
3. Wong S, Newman PJ, Best AS, Nairn KM, MacFarlane DR, Forsyth M (1998) J Mater Chem 8(10):2199–2203
4. Chen W, XU Q, Hu YS, Mai LQ, Zhu QY (2002) J Mater Chem 12:1926
5. Delmas C, Nadini A, Subeyrow JL (1999) Solid State Ionics 116:73
6. Kovacheva D, Nikolov V, Petrov K, Rojas RM, Herrero P, Rojo JM (2001) J Mater Chem 11:444–448
7. Chudnikova D (1971) J Inorg Mater 7:867
8. Gangadharan R, Kalaiselvi J, Shanmukaraj D (2002) J Alloys Compd 340:95–100
9. Annamma J, Devanarayanan S, Makoto Watanabe (2000) Spectrochim Acta Part A 56:877–885

10. Pikl R, de Waal D, Atiq A, Jazouli AEl (1998) Vib Spectro 16:137
11. Irvine JTC, Sinclair DC, West AR (1990) Adv Mater 2:38
12. Boukamp BA (1986) Solid State Ionics 20:301
13. Boukamp BA (1986) Solid State Ionics 18/19:136
14. Naddari T, Savariault JM, Feki HE, Salles P, Sahah AB (2002) J Solid State Chem 166:237–244
15. Almond DP, Duncan GK, West AR (1983) Solid State Ionics 8:159
16. Almond DP, West AR, Grant RJ (1982) Solid State Commun 44:1277
17. Almond DP, West AR (1983) Solid State Ionics 9/10:277
18. Rolling B (1998) Solid State Ionics 105:185
19. Vijayakumar M, Selvasekarapandian S (2002) Solid state ionics: trends in the new millennium. World Scientific, pp 599–604
20. Luo J, Almond DP, Stevens R (2003) J Am Ceram Soc 7:1703